The performance of maximum entropy methods in spectral deconvolution

M. W. Johnson and J. Lister
Rutherford-Appleton Laboratory
Chilton, Didcot, Oxon OX11, 0QX
UNITED KINGDOM

Introduction

There have been a number of previous demonstrations of the use of the Maximum Entropy principle (MaxEnt) in the deconvolution of experimental spectra [1-3]. However, as far as we know, there have been no previous discussions of the problems that arise in applying MaxEnt methods in practice. When deconvoluting a known, model spectrum it is straightforward to show, by means of an R-factor, that you have reached good agreement with the intrinsic spectrum. When deconvoluting real data the experimentalist derives a result, but then does not know how much credence to place on the result. The question 'what are the error bars' is not appropriate since the errors on a deconvoluted spectrum are not uncorrelated, but the spirit of the question is valid. This paper addresses itself to that problem.

Our approach is purely pragmatic. In the first section we show the results of deconvoluting a Gaussian line shape from three different intrinsic line shapes. This demonstrates not only the quality of the deconvoluted spectrum that may be obtained, but also how the final R-factor varies as a function of the Gaussian width.

In the second section the procedure is repeated for doublet intrinsic peaks, and the criteria for separation established.

In the third section we demonstrate that line shapes other than Gaussian may be removed from broadened spectra and examine the effects of uncertainties in our knowledge of the broadening function.

Finally we demonstrate the use of MaxEnt on a real problem where the technique has been used to substantially improve the resolution of an inelastic spectrometer.

THE DECONVOLUTION OF GAUSSIAN LINE SHAPES

In all the computer experiments described below the following procedure and definitions were used.

An intrinsic spectrum is defined, corresponding to the result that would be measured by an instrument with perfect resolution and no statistical error. This intrinsic spectrum is broadened by the resolution function and noise (with Poisson statistics) is added to produce the observed spectrum. The METRIC [4] MaxEnt method is then used to deconvolute the observed spectrum using the broadening function to yield the deconvoluted spectrum. Clearly the broadening function should be identical to the resolution function, if the deconvoluted spectrum is to agree with the intrinsic spectrum.

The first computer deconvolutions were conducted to enable users of the method on real data to estimate the likely difference between the deconvoluted spectrum and the (unknown) intrinsic spectrum. In these experiments three different intrinsic spectra were used :

$$\text{GAUSSIAN} \quad y = (1/\sigma\sqrt{2\pi})\, e^{-x^2/2\sigma^2} + b$$

$$\text{CAUCHY} \quad y = (1 + x^2/\lambda^2)/\pi\lambda + b$$

$$\text{GAMMA} \quad y = u^3x^2e^{-ux}/2 + b$$

Each were calculated over a time base from 0 to 1600 μs using channels of width 8 μs.

The tests were carried out with varying values for the background level (b) and different values for σ_r, the standard deviation of the Gaussian resolution function which was used to broaden the intrinsic spectra.

Figures 1 , 2 and 3 (A-C) show sample results for each of the three types of intrinsic spectra with the following parameters

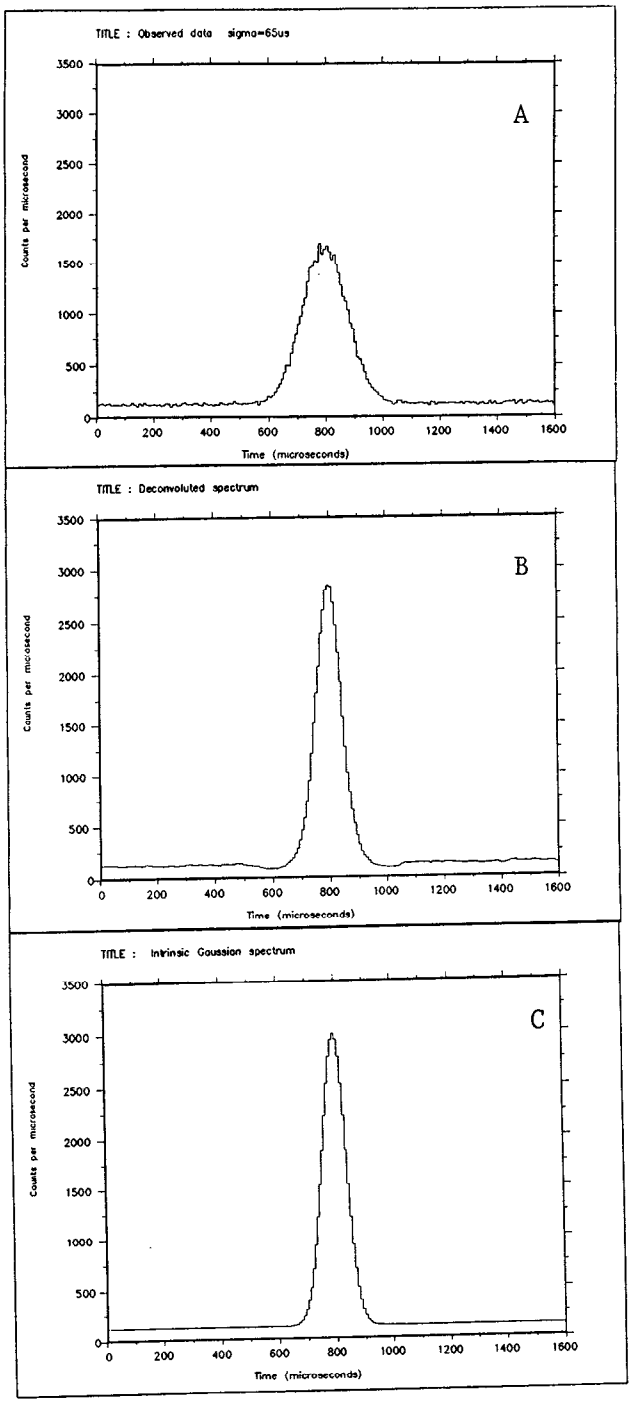
TITLE : Observed data sigma=65us
A
Counts per microsecond
Time (microseconds)
TITLE : Deconvoluted spectrum
B
Counts per microsecond
Time (microseconds)
TITLE : Intrinsic Gaussian spectrum
C
Counts per microsecond
Time (microseconds)

Figure 1

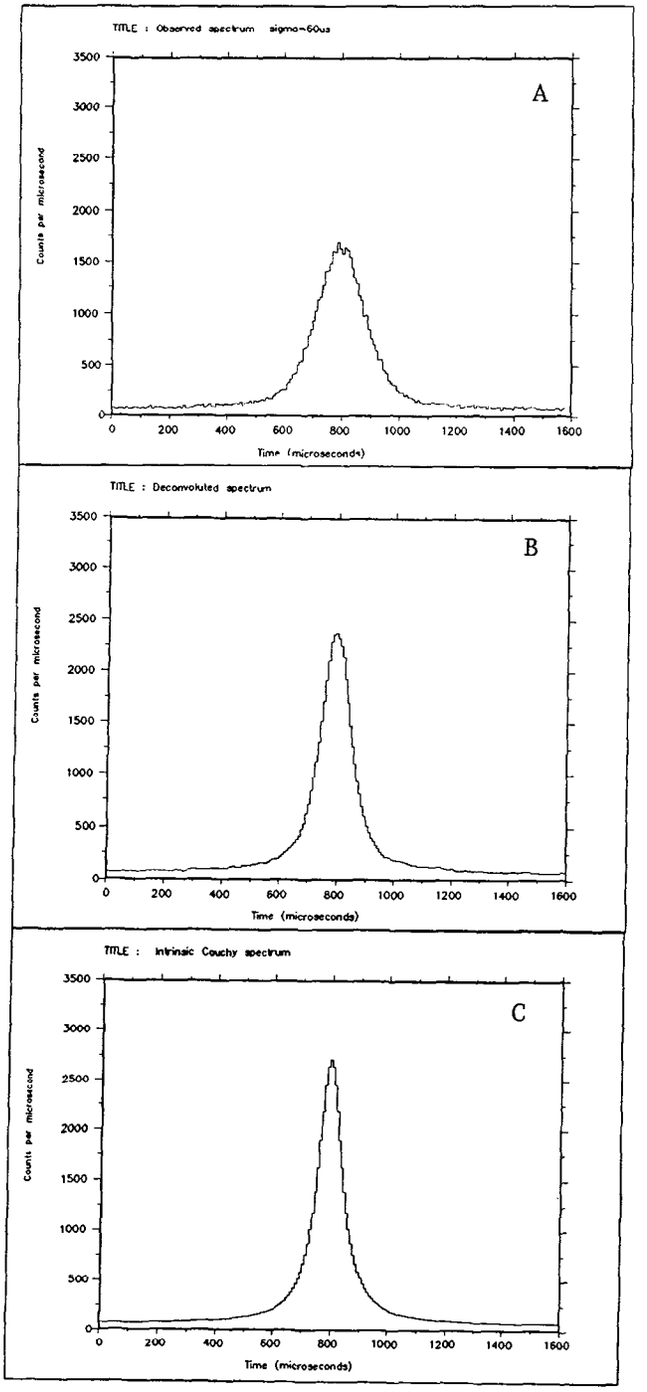
TITLE : Observed spectrum sigma=60us
A
Counts per microsecond
Time (microseconds)
TITLE : Deconvoluted spectrum
B
Counts per microsecond
Time (microseconds)
TITLE : Intrinsic Cauchy spectrum
C
Counts per microsecond
Time (microseconds)

Figure 2

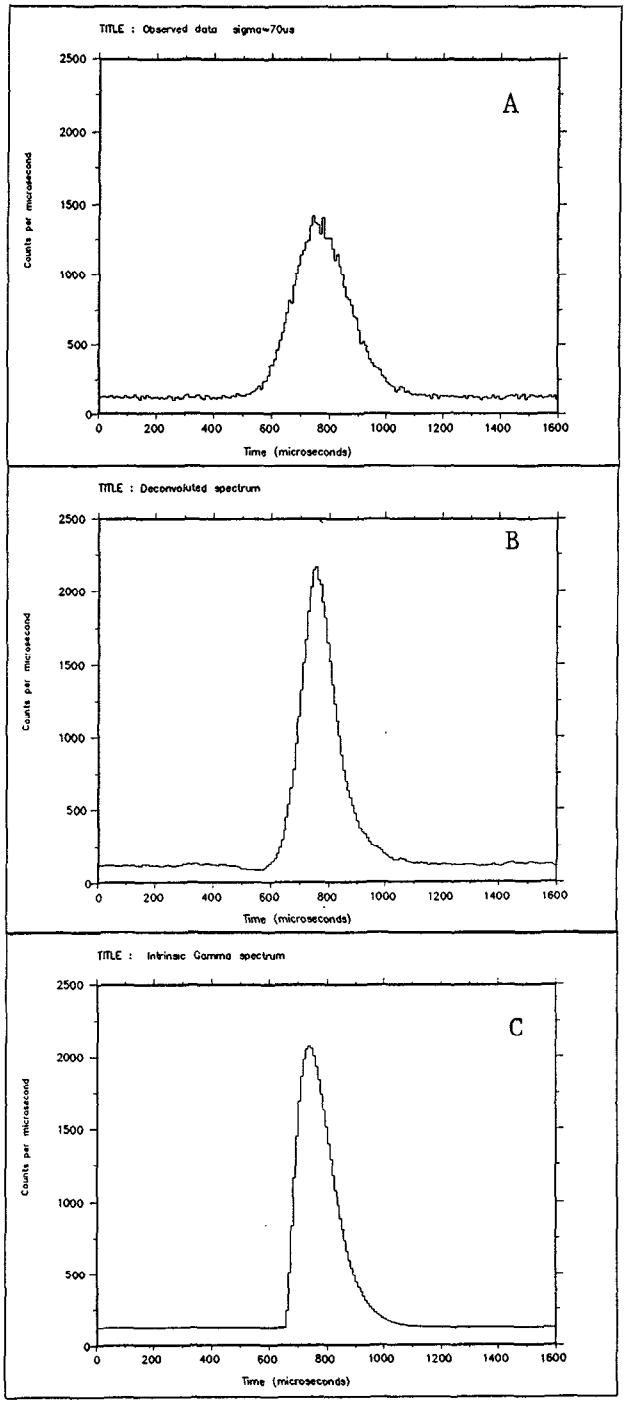
TITLE : Observed data sigma=70us
A
Counts per microsecond
Time (microseconds)
TITLE : Deconvoluted spectrum
B
Counts per microsecond
Time (microseconds)
TITLE : Intrinsic Gamma spectrum
C
Counts per microsecond
Time (microseconds)

Figure 3

	Intrinsic	FWHM (μs) intrinsic	σ_r (μs)	Background
Figure 1	Gaussian	100	65	0.4
2	Cauchy	100	60	0.2
3	Gamma	140	70	0.4

The background is expressed as an area fraction of the total area.

In these figures A is the observed spectrum, B is the deconvoluted spectrum and C the intrinsic spectrum.

Defining the R-factor as :

$$R^2 = \frac{\Sigma\ (d_i - i_i)^2}{\Sigma\ i_i^2}$$

where d_i is the deconvoluted spectrum

i_i is the intrinsic spectrum

We may plot R as a function of $\sigma_r/FWHMH_{obs}$, assuming $\sigma_r/FWHMH_{obs}$ to be a measure of the 'difficulty' of the deconvolution. This is done in Figures 4, 5 and 6. It will be seen from these plots that :

(a) The results are largely independent of the background level.

(b) There is a general similarity between the R-factors when deconvoluting all peak shapes - especially those of Cauchy and Gamma distributions.

(c) If the deconvolution problem lies in the range $0 < \sigma_r/FWHMH_{obs} < 0.2$ the final R -factor will be < 5%.

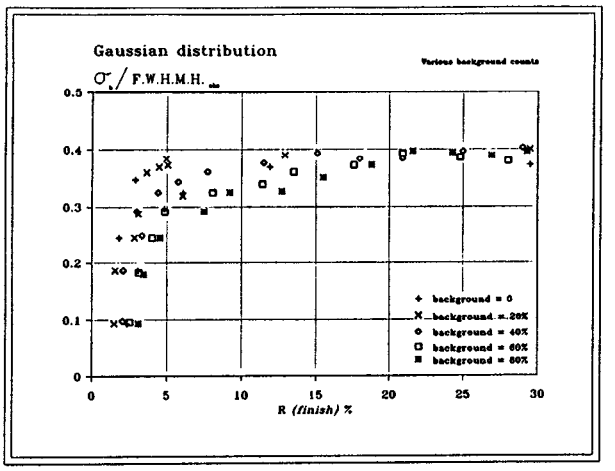

Figure 4

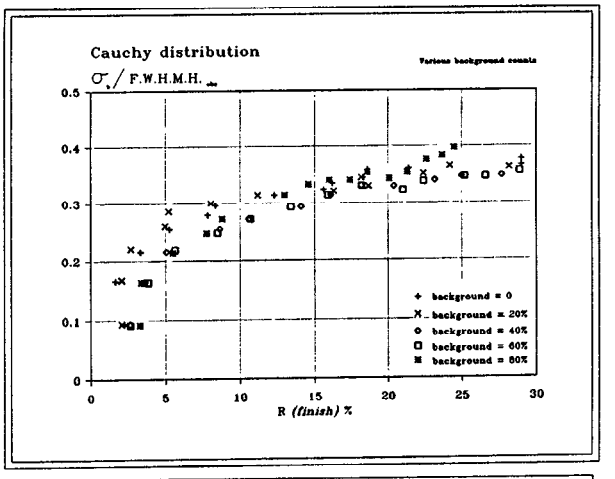

Figure 5

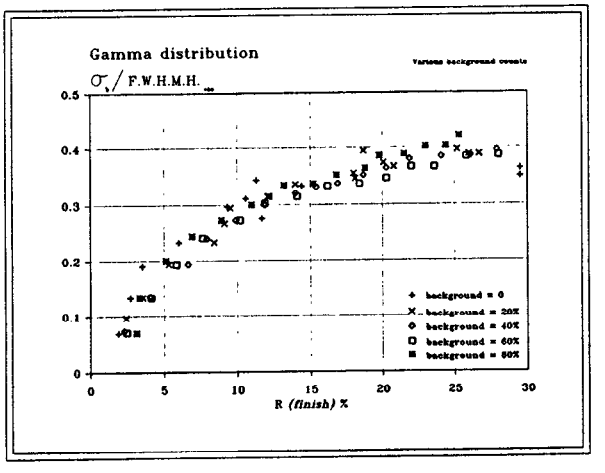

Figure 6

These results are useful in giving us confidence when deconvoluting peaks in this region. It also demonstrates that the method becomes unstable for $\sigma_r/FWHMH_{obs}$ ratios greater than 0.30 when the resolution function is Gaussian.

2. DOUBLET INTRINSIC PEAK SHAPES

The second series of tests used two peaks with a background count at a constant 20% of the total count, with σ_r in the range 10-80 μs, and the separation between the peaks in the range 80-300 μs.

Figures 7, 8 and 9 (A-C) show sample results for the following parameters :

Figure	i	$FWHMH_i$ (μs)	σ_r (μs)	Separation (μs)
7	Gaussian	100	60	132
8	Cauchy	100	60	165
9	Gamma	140	60	148

The R-factor results for the double peak deconvolutions are shown in Figures 10, 11 and 12. This shows the R-factor versus the peak separation for various values of σ_r. The results to the left of the vertical line on each Figure are those for which the two peaks are not resolved.

Again it becomes clear that there is a broad agreement of the region where separation will occur and the R-factors exhibit predictable, systematic variations which should be useful in indicating the likely results to be obtained when deconvoluting true experimental data.

3. NON GAUSSIAN RESOLUTION FUNCTIONS

In all the preceding experiments the resolution function has been Gaussian.

Figures 13-17 (A-D) show sample plots of results obtained using single and double peak intrinsic Gaussian

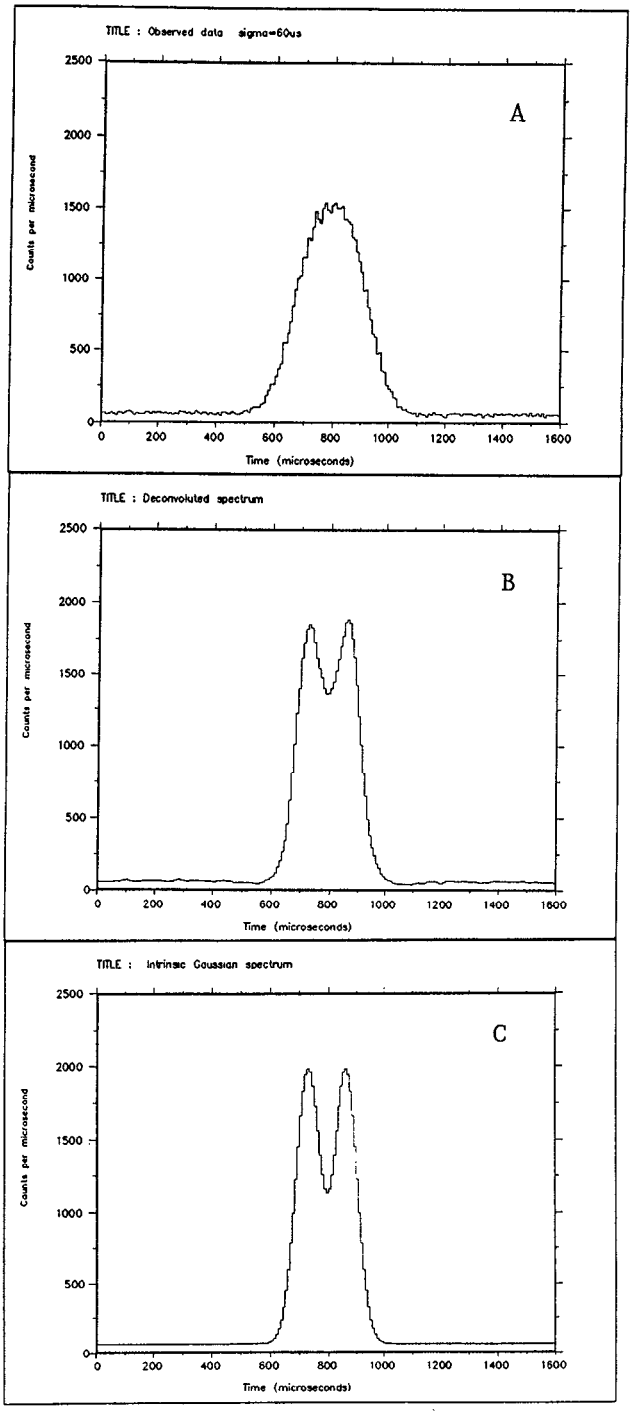
TITLE : Observed data sigma=60us
A
Counts per microsecond
Time (microseconds)
TITLE : Deconvoluted spectrum
B
Counts per microsecond
Time (microseconds)
TITLE : Intrinsic Gaussian spectrum
C
Counts per microsecond
Time (microseconds)

Figure 7

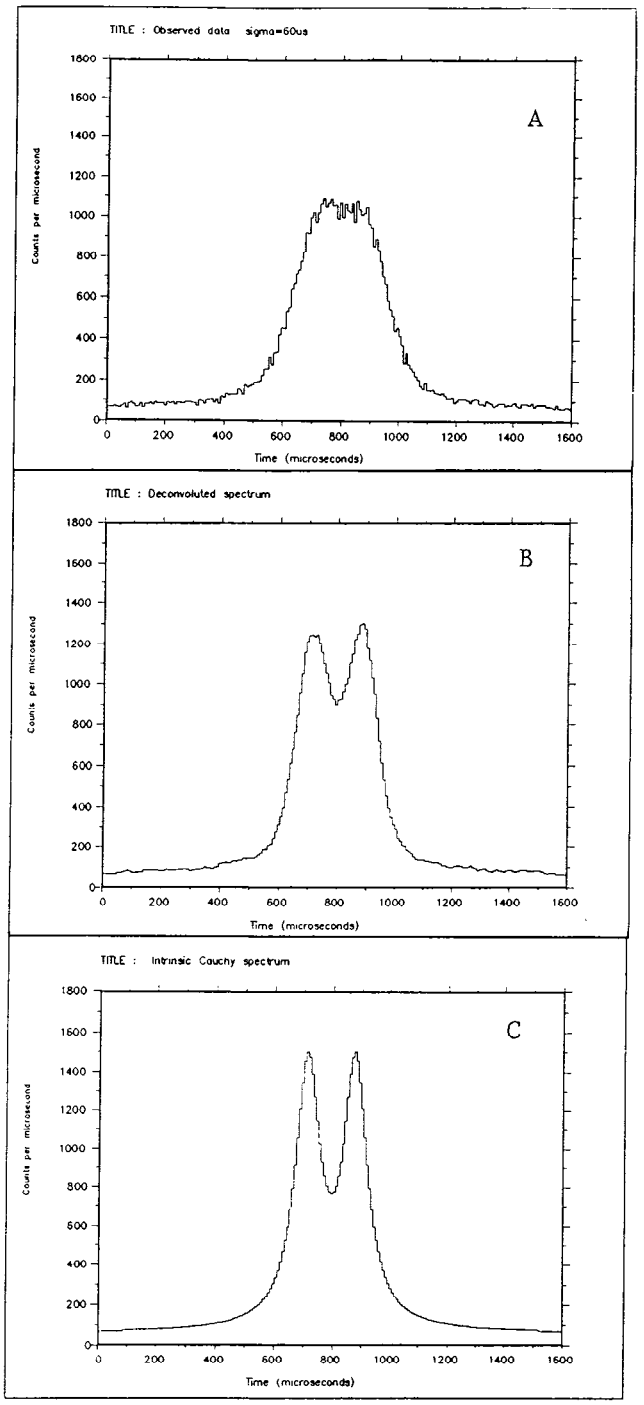
TITLE : Observed data sigma=60us
A
Counts per microsecond
Time (microseconds)
TITLE : Deconvoluted spectrum
B
Counts per microsecond
Time (microseconds)
TITLE : Intrinsic Cauchy spectrum
C
Counts per microsecond
Time (microseconds)

Figure 8

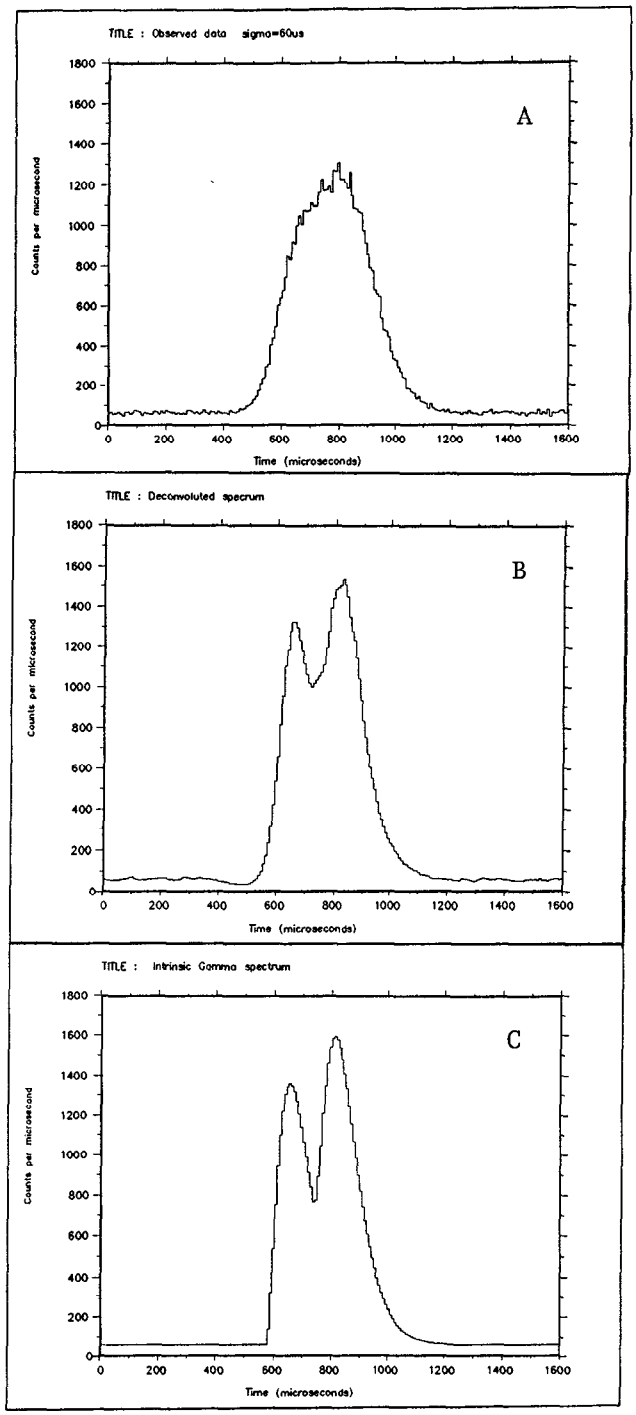
TITLE : Observed data sigma=60us
A
Counts per microsecond
Time (microseconds)
TITLE : Deconvoluted specrum
B
Counts per microsecond
Time (microseconds)
TITLE : Intrinsic Gamma spectrum
C
Counts per microsecond
Time (microseconds)

Figure 9

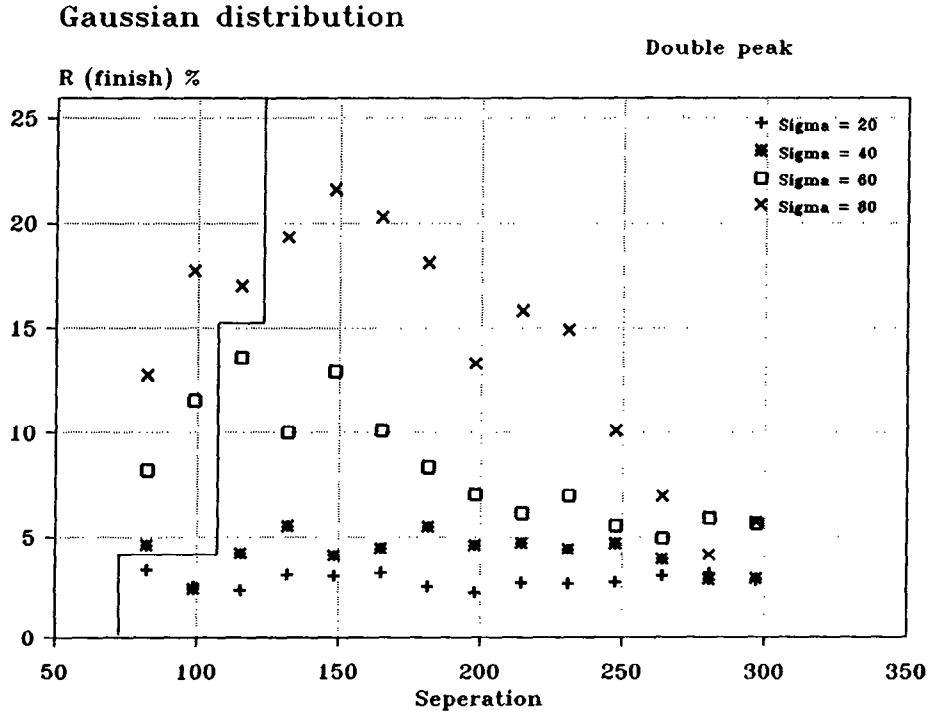
Gaussian distribution
Double peak
R (finish) %
25
20
15
10
5
0
50
100
150
200
250
300
350
Seperation
Sigma = 20
Sigma = 40
Sigma = 60
Sigma = 80

Figure 10

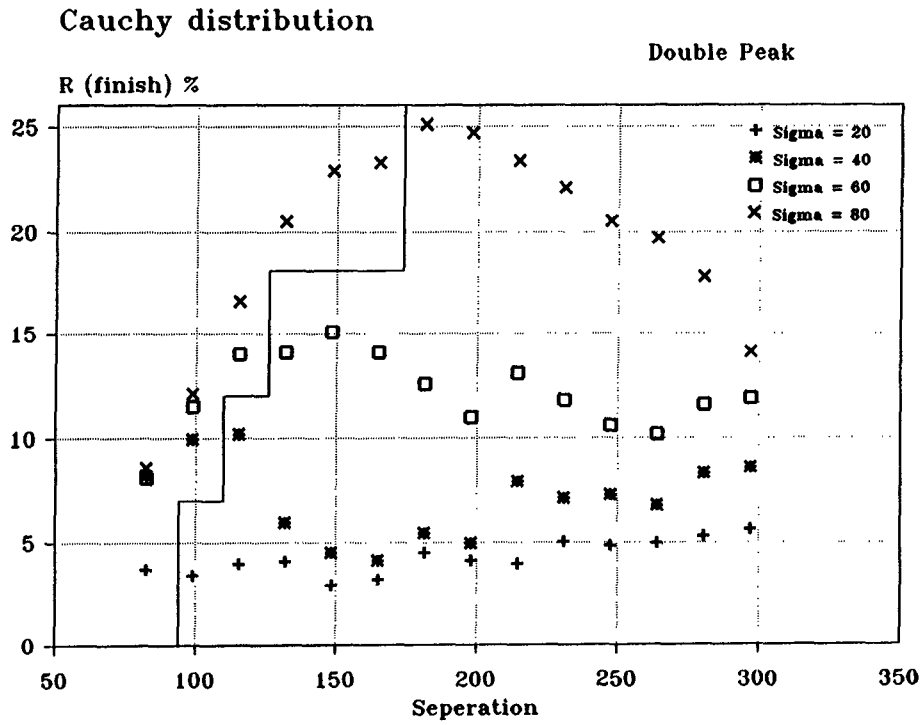
Cauchy distribution
Double Peak
R (finish) %
25
20
15
10
5
0
50
100
150
200
250
300
350
Seperation
Sigma = 20
Sigma = 40
Sigma = 60
Sigma = 80

Figure 11

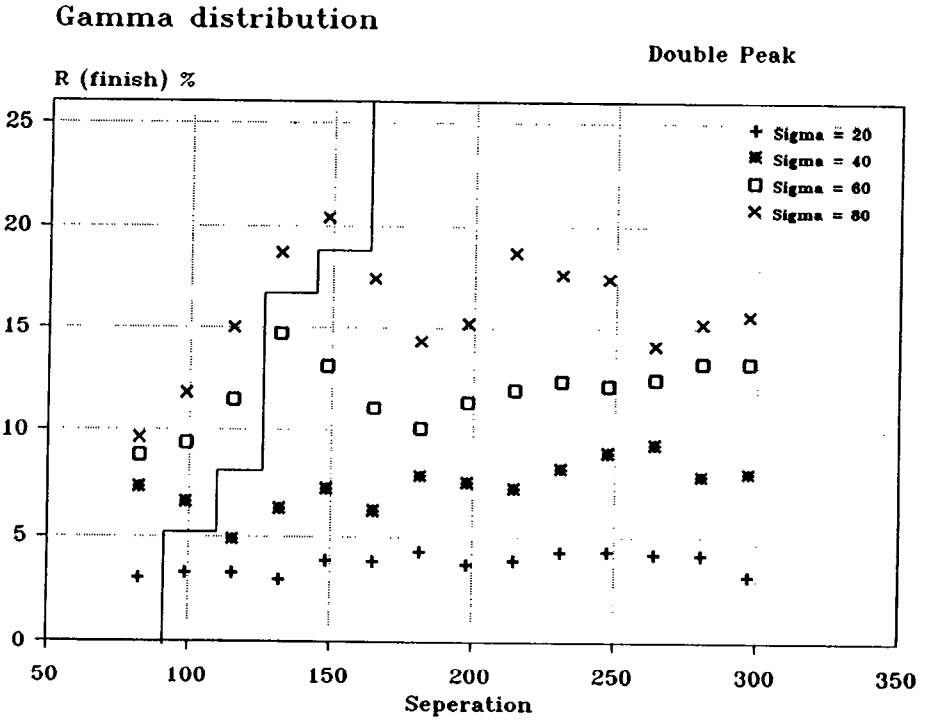
Gamma distribution
Double Peak
R (finish) %
25
20
15
10
5
0
50
100
150
200
250
300
350
Seperation
Sigma = 20
Sigma = 40
Sigma = 60
Sigma = 80

Figure 12

distributions, and Gamma or Cauchy resolution functions. In Figures 13-17, A is the observed data, B is the resulting deconvolution, C is the resolution function and D is the intrinsic spectrum.

Fig.	No. of Peaks	Sep. (μs)	$FWHM_i$	$FWHM_r$	Broadening Function
13	1	-	3.0	17.0	Gamma
14	1	-	6.0	11.0	Gamma
15	1	-	5.0	14.0	Cauchy
16	2	6.0	3.0	11.0	Gamma
17	2	10.0	8.0	11.0	Gamma

In all five cases, the total count was 60,000 (for the intrinsic spectra). For the single peak plots, a background count of 33% of the total count was included. The double peak plots had no background.

The results from the double peak deconvolution (Figures 16, 17) are quite remarkable, showing the separation of identifiable peaks even when the width of the resolution function is comparable with the peak separation. This success may be due to the absence of background.

4. EFFECTS OF UNCERTAINTY IN THE KNOWLEDGE OF σ_r

When experimental spectra have to be deconvoluted (as opposed to computer simulated spectra) there may be some uncertainty in the knowledge of σ_r, since this cannot in many cases be directly measured. We therefore investigated the effect of this uncertainty by deconvoluting the observed spectra with a range of different broadening functions.

The results of these trials are given in Tables 1, 2 and 3. It will be seen that, as expected, an underestimate of the broadening function causes no serious problem and a solution ($\chi^2 \leq 1$) is found. If the broadening function is overestimated by more than ~ 10% no solution is found.

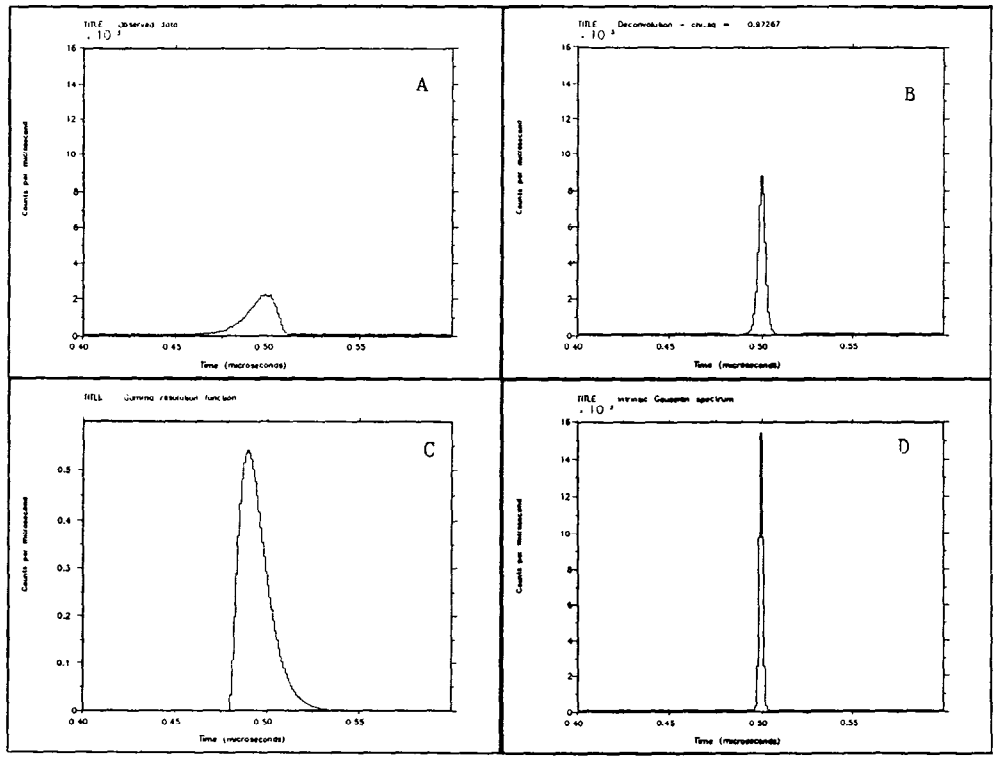

Figure 13

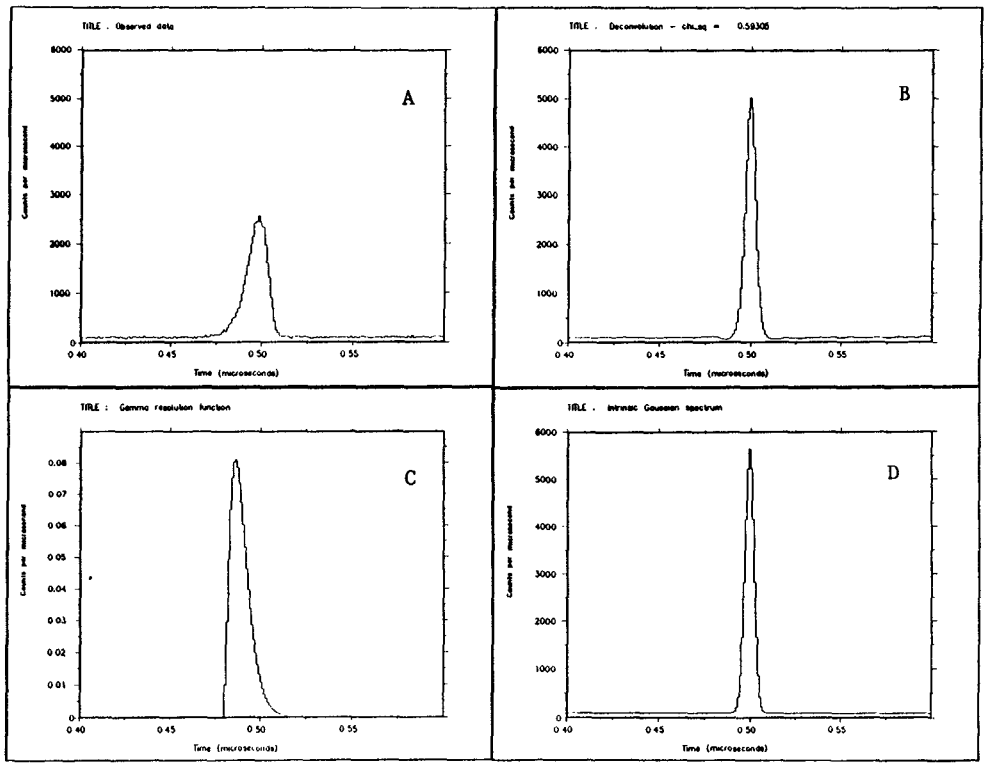

Figure 14

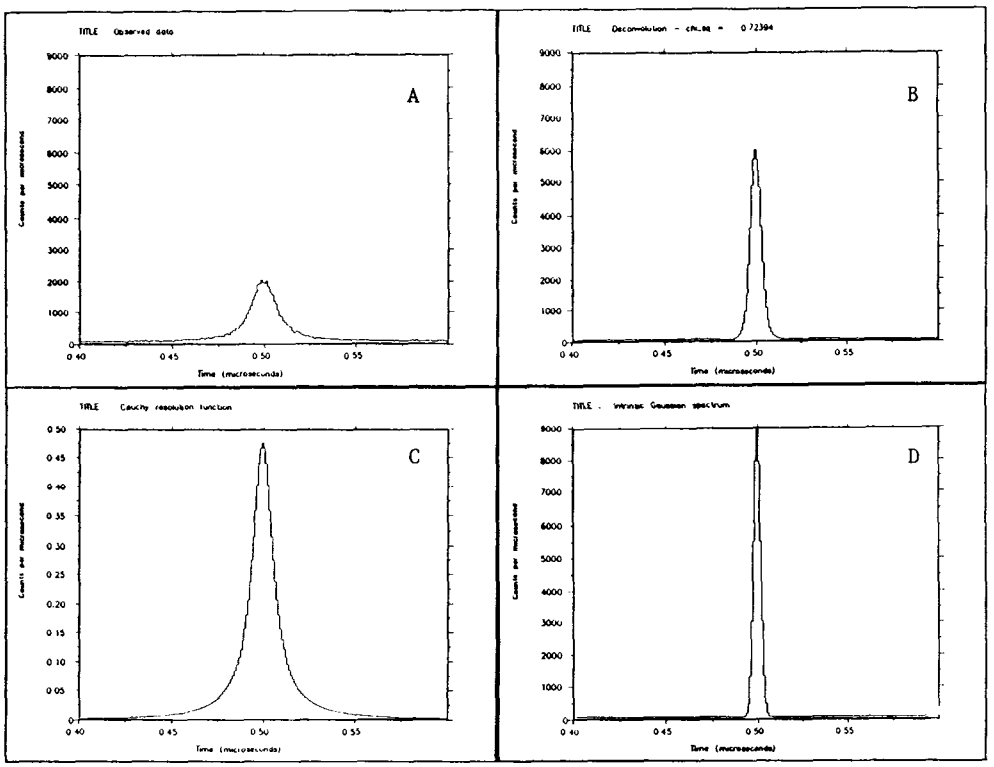

Figure 15

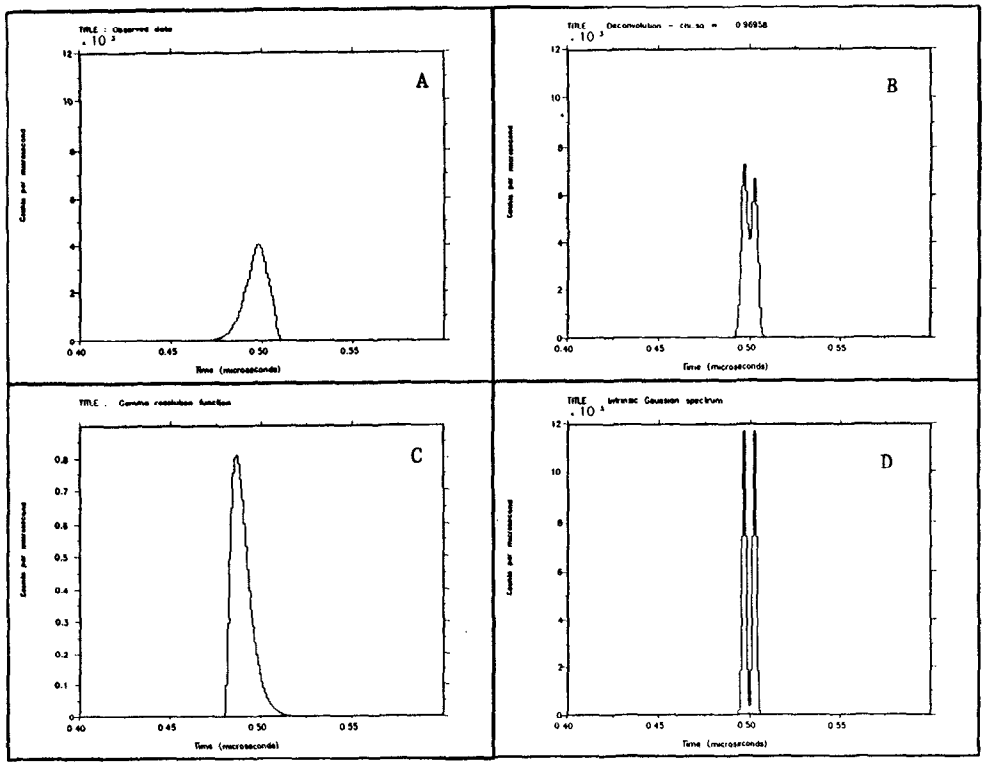

Figure 16

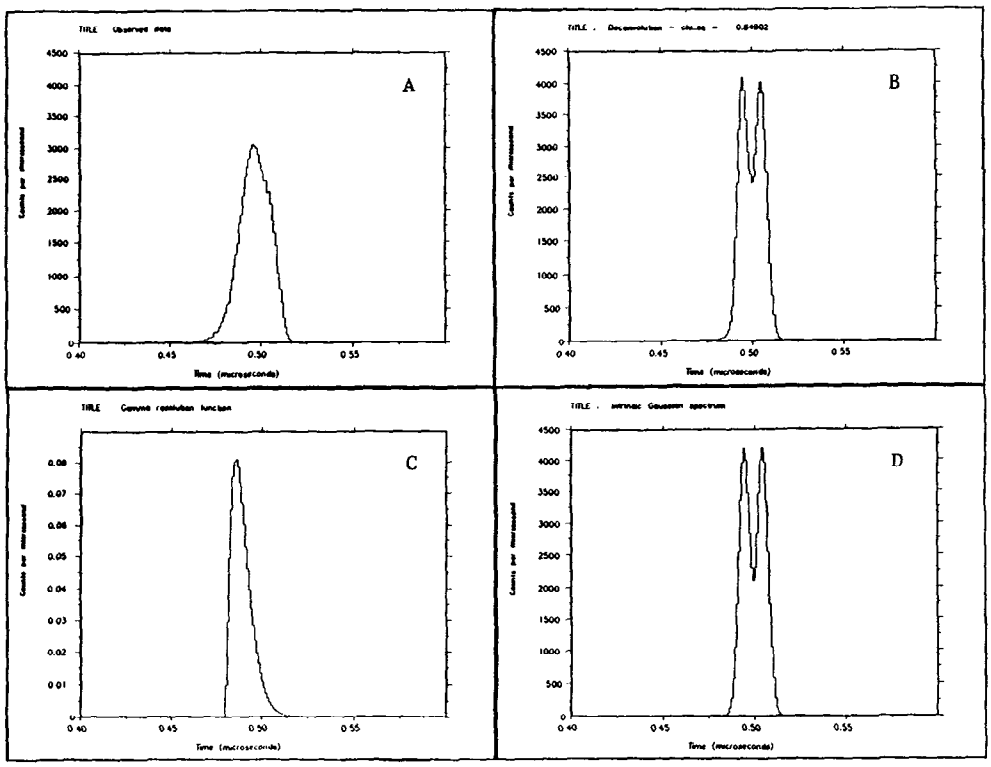

Figure 17

TABLE 1

Intrinsic : Gaussian
$FWHMH_i$: 9.4
Resolution : Gamma
$FWHMH_r$: 11.0
Background : 0.0

Broadening FWHMH	χ^2	Iterations	Solution
15.0	708	600	x
14.0	402	600	x
13.0	230	700	x
12.0	< 1	900	√
11.0*	< 1	500	√
10.0	< 1	500	√
9.0	< 1	400	√

TABLE 2

Intrinsic	:	Gaussian
$FWHMH_i$	:	5.9
Resolution	:	Gamma
$FWHM_R$	:	11.0
Background	:	0.33

Broadening FWHMH	χ^2	Iterations	Solution
15.0	8.4	20,000	x
14.0	4.3	20,000	x
13.0	< 1	1,800	√
12.0	< 1	1,000	√
11.0*	< 1	700	√
10.0	< 1	600	√
9.0	< 1	400	√

TABLE 3

Intrinsic	:	Gaussian Doublet
$FWHMH_i$	:	7.1
Separation	:	10.0
Resolution	:	Gamma
$FWHM_R$	:	11.0
Background	:	0.0

Broadening FWHMH	χ^2	Iterations	Solution
14.0	5.2	20,000	x
13.0	1.6	20,000	x
12.0	< 1	1,700	√
11.0	< 1	1,300	√
10.0	< 1	1,000	√
9.0	< 1	800	√
9.0	< 1	800	√

The χ^2 rapidly diverges as the broadening FWHMH is increased beyond the 'true' value. In fact it is possible that, in the absence of any other information, this behaviour could be used to try to judge the width of the broadening function.

5. TEST ON EXPERIMENTAL DATA

So far all the results discussed in this paper have been for computer simulated spectra. As a test of the method the algorithm was applied to data recorded on the IRIS spectrometer at the ISIS facility. The raw data is shown in Figure 18. and was obtained from a sample of 4-methyl pyridine. If the CH_3 group in this molecule were a free rotator the spectrum would consist of a single line, broadened by the instrumental resolution.

In fact three peaks are easily seen and the deconvolution of the observed data (Figure 19) by a Gaussian broadening function (σ_b = 0.0064 meV) suggests that a fourth peak is in fact present as a shoulder to the central peak. This is agreement with the presence of four molecules in the unit cell.

6. CONCLUSION

In this paper we have explored some of the issues that will have to be resolved if the MaxEnt method is to become a standard data analysis tool. The central problem hinges on the confidence levels to be assigned to the result, either when the broadening function is known precisely or when there may be some systematic error in its assumed value.

Since these confidence limits cannot be determined analytically the only method at present available is the empirical one. If one is deconvoluting a particular experimental spectrum the result can be used as the starting point of a series of computer experiments to determine the stability of the solution to a number of random or systematic errors.

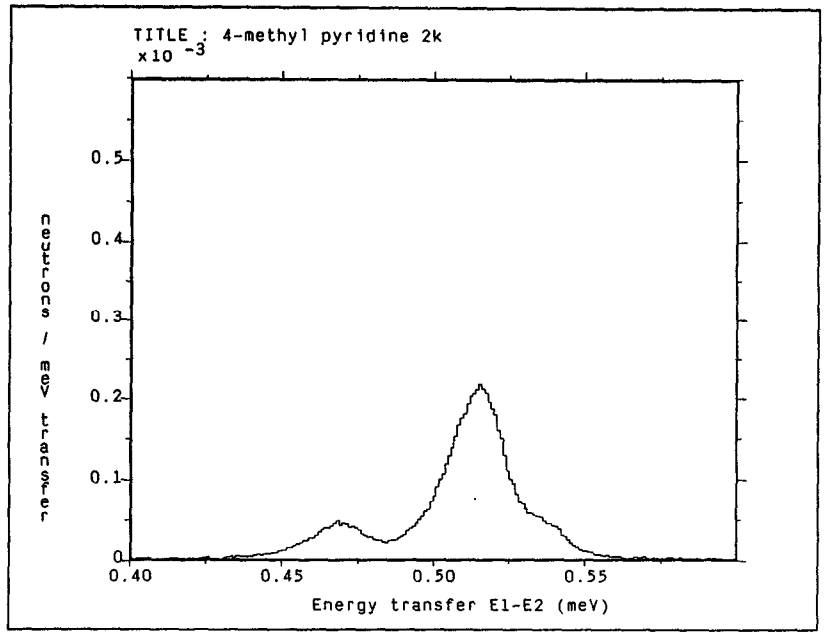

Figure 18

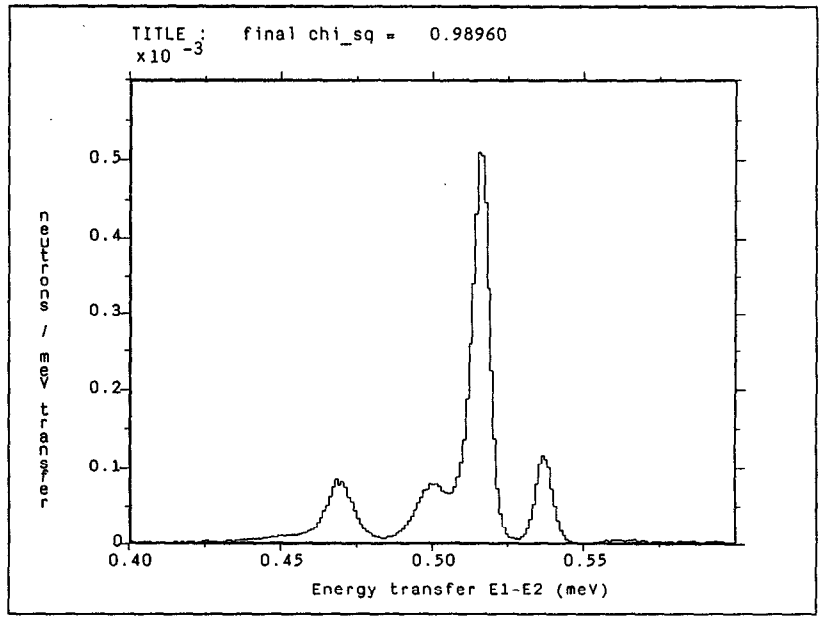

Figure 19

References

1. Burg J P (1967) Maximum-Entropy Spectral Analysis, Conf Paper reprinted in: Modern Spectrum Analysis, Ed D G Childers (New York, Wiley 1978)

2. Gull S F and Daniel G J (1978) Nature 272 686-90

3. Steinstrup S (1986) Conf Paper in: Neutron Scattering Data Analysis, Ed M W Johnson (IOP Conference Series 81 1986)

4. Johnson M W (1987) Rutherford Appleton Laboratory Report RAL-87-058